**Proceedings of the ECCOMAS Thematic International Conference on
Simulation and Modeling of Biological Flows (SIMBIO 2011)
September 21–23, 2011, VUB, Brussels, Belgium**

An Energy Absorbing Layer for the Structure Outflow Boundary Applied to 2D Heart Valve Dynamics with Multiple Structures.

Thomas Wick*

1 Institute of Applied Mathematics,
University of Heidelberg
INF 293/294, 69120 Heidelberg, Germany,
thomas.wick@iwr.uni-heidelberg.de

Abstract

In valve-blood-wall interactions, the radius of the blood vessel wall may vary by up to ten percent. This structural displacement is quite large, leading to difficulties at the artificial boundaries of the computational domain. In this work, we investigate the dynamical behavior of the aortic heart valve and we introduce a technique that absorbs structural energy and prevents the back flow of structure waves at the outflow. To this end, the computational domain is prolonged by an artificial layer on which we solve a damped version of the hyperbolic structure equations. The coupling of fluid and structure equations is realized by a monolithic solution algorithm, where the fluid equations are rewritten in the 'arbitrary Lagrangian Eulerian' framework. The structure is divided into different parts to account for the different physical properties of tissue of the heart, the valves, and the aorta. Specifically, we are dealing with varying structure coefficients and different constitutive tensors. We present numerical examples that substantiate the performance of our techniques.

Keywords: finite elements, fluid-structure interaction, Arbitrary Lagrangian Eulerian method, stability, damped wave equation

Introduction

Cardiovascular diseases represent a major fraction of mortalities in industrialized countries. For this reason, there is an increasing demand from the medical community for rigorous and quantitative investigations of the human cardiovascular system [1]. However, the complexity of the circulatory system makes modeling and simulation challenging because there are many fundamental factors that must taken into account.

In this work, we focus on the main component of the circulatory system: the heart. More specifically, we are interested in the modeling and the simulation of the aortic heart valve, which pumps oxygenated blood from the left ventricle into the aorta. This arrangement implies that there is an interaction between the blood, the heart walls and the vessel walls. The mathematical approach of choice to construct an appropriate model and simulation of these dynamics is the fluid-structure interaction method. Beyond this approach, fluid-structure interactions have significant influences in bio-mechanics [1–4].

Various approaches to model heart valve dynamics exist. Usually, these approaches are considered as fluid-structure interaction problems that can be solved by different solution algorithms [5–9]. Here, we use the 'arbitrary Lagrangian-Eulerian' framework (ALE), which is frequently used in the literature.

We solve the problem by a monolithic solution algorithm (see [10–14]) because one must overcome the well-known added-mass effect that occurs when the density of a fluid and a structure are of the same order, such as in hemodynamics [15]. In addition, a closed setting for the equations is necessary for rigorous goal-oriented error estimation [16].

By construction, the ALE approach is not capable of modeling topological changes, which occur when two valves touch each other. This could be achieved, for instance, with the immersed boundary method [7], the Fictitious Domain method [17], or with a fully Eulerian approach [13]. However, this point is of less importance in our studies, because we focus on boundary conditions for the structure of the outflow section. This issue should not be neglected because the radius of the aorta may vary in a range of $5 - 10$ percent between diastole and systole (the two phases in a cardiac cycle) [1]. This is a large displacement of the blood vessel wall that effects both the flow field and the blood vessel dynamics.

In recent years, much effort has been spent on modeling appropriate descriptions for fluid and pressure conditions on the artificial outflow boundary [4, 18–21]; these descriptions are related to the flow field. Consideration of appropriate structural conditions becomes important when dealing with the large deflections of the blood vessel walls.

Specifically, we are interested in the capability to absorb outgoing waves (i.e., energy) to prevent the back flow of waves.

To the best of our knowledge, this topic is novel, and others have only just begun with investigations [22]. Here, the authors consider the flow rate conditions of the fluid problem and a complete set of (non-defective) boundary conditions for the structure problem on the artificial outflow section.

Originally, energy absorption problems drew attention in acoustic and electromagnetic wave propagation analysis [23, 24]. The main difficulty is, that the standard Dirichlet and Neumann boundary conditions are not able to absorb energy from outgoing waves. As a result, various approximate boundary conditions have been used to absorb incoming waves. One approach to eliminating reflections was suggested by appending an artificial layer to the computational domain. This layer is intended to absorb the waves. Specifically, one can use a perfectly matched layer (PML) [25]. We employed this idea to extend the computational domain that is used to absorb the outgoing waves in our fluid-structure interaction problem. The major disadvantage of this approach is the increased computational cost due to solving both the complete fluid equations and the structure equations on an artificial domain. To overcome this drawback, we could solve reduced equations in the artificial layer or we would use an initial, coarser mesh in the artificial part. We employed the latter strategy to deal with the drawback, and we coarsened the initial mesh by hand in that region.

The last issue that will be studied in this work, accounts for the different physical properties of the structures (namely the tissue) of the heart, the valves, and the aorta. To this end, we use two strategies. First, we use the same constitutive material model but with varying coefficients to run the simulations. Second, we upgrade our solution algorithm while using two different constitutive structure tensors. This verification has important consequences for future applications and more detailed modeling of arterial tissue, for instance.

This contribution is organized as follows: In Section *The Fluid-Structure Problem*, we describe the equations for both the fluid and the structure, including a damped hyperbolic equation. The proposed method is stable on the continuous level. Afterwards, we formulate the problem in a monolithic setting. Section *Discretization* is devoted to a brief description of the discretization process. In addition, we state a stabilization technique for the convective term that is based on streamline diffusion. In the last section, we exemplify our proposed method by presenting prototypical numerical examples. The parameters for both the material and the geometry are taken from the literature. The computations are performed with the numerical software library deal.II [26].

The Fluid-Structure Problem

We denote by $\Omega \subset \mathbb{R}^d$, $d = 2, 3$, the domain of the fluid-structure interaction problem. This domain is supposed to be time independent but consists of two time dependent sub-domains $\Omega_f(t)$ and $\Omega_s(t)$. The interface between both domain is denoted by $\Gamma_i(t) = \partial\Omega_f(t) \cap \partial\Omega_s(t)$. The initial (or later reference) domains are denoted by $\widehat{\Omega}_f$ and $\widehat{\Omega}_s$, respectively, with the interface $\widehat{\Gamma}_i$. Further, we denote the outer boundary with $\partial\widehat{\Omega} = \widehat{\Gamma} = \widehat{\Gamma}_D \cup \widehat{\Gamma}_N$ where $\widehat{\Gamma}_D$ and $\widehat{\Gamma}_N$ denote Dirichlet and Neumann boundaries, respectively.

We adopt standard notation for the usual Lebesgue and Sobolev spaces [27]. We use the notation $(\cdot,\cdot)_X$ for a scalar product on a Hilbert space X and $\langle\cdot,\cdot\rangle_{\partial X}$ for the scalar product on the boundary ∂X. Specifically, we define $H_0^1(X) = \{v \in H^1(X) : v = 0 \text{ on } \Gamma_D \subset \partial X\}$. We will use the short notation $\hat{V}_X := H^1(X)$, $\hat{V}_X^0 := H_0^1(X)$ and $\hat{L}_X := L^2(X)$, $\hat{L}_X^0 := L^2(X)/\mathbb{R}$. For the time-dependent problems, we define a time interval $I := [0, T]$ with the end time value $T < \infty$.

We expect that the reader is familiar with continuum mechanics and we omit differentiation between scalar-valued spaces (and variables) and their vector-valued extensions.

In the following, we study the interaction of an incompressible Newtonian fluid and a structure of hyperbolic type [19]. The equations for fluid and structure are defined in their natural frameworks. The fluid problem reads in $\Omega_f(t)$:

$$\begin{aligned} \rho_f\, \partial_t v_f|_{\hat{\mathcal{A}}} + \rho_f(v_f - w)\cdot\nabla v_f - \mathrm{div}\sigma_f &= 0 \\ \mathrm{div} v_f &= 0 \\ v_f = v^D \quad \text{on } \Gamma_{f,\mathrm{in}}(t), \quad \sigma n_f = g_{f,N} \quad \text{on } \Gamma_{f,N}(t), & \end{aligned} \tag{1}$$

with the Cauchy stress tensor σ_f. The (undamped) structure problem is defined by:

$$\begin{aligned} \hat{\rho}_s\partial_t^2\hat{u}_s - \widehat{\mathrm{div}}(\widehat{F}\widehat{\Sigma}_s) &= 0 \quad \text{in } \widehat{\Omega}_s, \\ \hat{u}_f = 0 \quad \text{on } \widehat{\Gamma}_{s,D}, \quad \widehat{F}\widehat{\Sigma}_s\hat{n}_s &= 0 \quad \text{on } \widehat{\Gamma}_{s,N}, \end{aligned} \tag{2}$$

with the second Piola-Kirchhoff tensor $\widehat{\Sigma}_s$ and the deformation gradient $\widehat{F} = I + \widehat{\nabla}\hat{u}$, where I denotes the identity tensor. The coupling conditions are given by (with $\det(\widehat{F}) = \hat{J}$):

$$\hat{v}_f = \hat{w} \text{ on } \widehat{\Gamma}_i, \tag{3}$$

$$\hat{J}\widehat{\sigma}_f\widehat{F}^{-T}\hat{n}_f + \widehat{F}\widehat{\Sigma}_s\hat{n}_s, = 0 \text{ on } \widehat{\Gamma}_i, \tag{4}$$

where $\hat{w}$ denotes the fluid domain velocity that can be constructed by $\hat{w} = \partial_t\hat{u}_s$ on $\widehat{\Gamma}_i$. The stress tensors, $\widehat{\sigma}_f$ and $\widehat{\Sigma}_s$, will be specified below. The viscosity and the density of the fluid are denoted by ν_f and ρ_f, respectively. The elastic structure is characterized by the Lamé coefficients μ_s, λ_s.

The physical unknowns are the (vector-valued) fluid velocity $\hat{v}_f : \widehat{\Omega}_f \times R^+ \to R^3$, the (scalar) fluid pressure $\hat{p} : \widehat{\Omega}_f \times R^+ \to R$, and the (vector-valued) structure

displacement $\hat{u}_s : \widehat{\Omega}_s \times R^+ \rightarrow R^3$. The ALE mapping is denoted by $\hat{\mathcal{A}} : \widehat{\Omega} \rightarrow \Omega(t)$ and is constructed from the displacements of the moving interface, i.e., $\hat{u}_f = \text{Ext}(\hat{u}_s|_{\widehat{\Gamma}_i})$. This condition is used to solve an additional partial differential equation that is explained below. Furthermore, any function $\hat{q} \in \widehat{\Omega}$ is defined on Ω by $q(x) = \hat{q}(\hat{x})$ with $x = \hat{\mathcal{A}}(\hat{x}, t)$.

Coupling conditions for multiple structures

To extend the standard fluid-structure interaction problem for the in-cooperation of multiple structures, we first recall the coupling conditions:

$$\begin{aligned} \hat{u}_{s,1} &= \hat{u}_{s,2} \quad \text{on } \widehat{\Gamma}_i, \\ \widehat{F}\widehat{\Sigma}_{s,1} &= \widehat{F}\widehat{\Sigma}_{s,2} \quad \text{on } \widehat{\Gamma}_i. \end{aligned} \tag{5}$$

In a variational framework, the second coupling condition in Equation (5) becomes an implicit condition. The Dirichlet-like condition of Equation (5) is strongly imposed in the corresponding Sobolev space.

The multi-structure models become important when considering a prototypical heart valve simulation. Here, we describe all structure parts (the section of the heart, the valves, and the aorta) by the same material model but with varying coefficients. These are unsteady on the interface where the different structures touch each other. We do not expect difficulties by using different constitutive models for the different structure parts. Its verification is important because one is interested in modeling blood vessels with more sophisticated material models [31, 32]. But, in contrast to the coupling of fluids and structures together, where the Cauchy stress tensor changes entirely, this kind of coupling is of a lower level, because the stress tensors have similar meaning and should not cause any difficulties. We address this subject in a numerical example below, where this assumption will be established.

However, the introduced structure models in this work, are not sufficient to obtain quantitative correctness of the wall stresses [19, 30, 31]. This limitation is because residual stresses (that are present in complex structures in biological tissues with composite reinforced fibers) can not be represented by these models. To represent residual stresses, more elaborated models are required [30–33]. Nevertheless, the STVK model permits us to study the numerical correctness of the proposed formulation and to validate the model.

Construction of the ALE mapping

The fluid mesh motion is constructed by posing an additional equation, which is driven by the motion of the interface $\Gamma_i(t)$, i.e., $\hat{\mathcal{A}} = \hat{u}_s$ on $\widehat{\Gamma}_i$, leading to $\hat{w} = \hat{v}_s$ on $\widehat{\Gamma}_i$. Further, we fix the inlet and the outlet boundary parts by $\hat{u}_f = 0$ on $\widehat{\Gamma}_{f,\text{in}}(\text{at left}) \cup \widehat{\Gamma}_{f,\text{out}}(\text{at right})$ (see Figure 1). In the fluid domain $\widehat{\Omega}_f$, the transformation $\hat{\mathcal{A}}$ is arbitrary but should satisfy certain regularity conditions (C^1-diffeomorphism) [19]. Specifically, the fluid mesh is constructed by solving a biharmonic equation (for large mesh deformations without re-meshing):

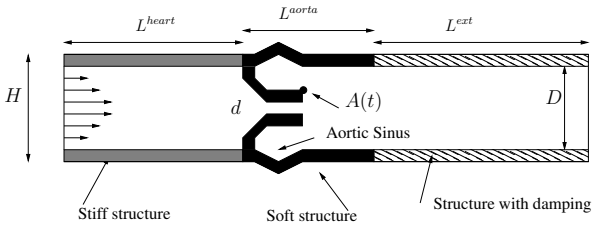

Figure 1 Configuration for the numerical examples.

$$\begin{aligned} \Delta^2 \hat{u}_f &= 0 \quad \text{in } \widehat{\Omega}_f, \\ \hat{u}_f &= 0 \quad \text{on } \widehat{\Gamma}_{f,\text{in}} \cup \widehat{\Gamma}_{f,\text{out}}, \\ \partial_n \hat{u}_f &= 0 \quad \text{on } \widehat{\Gamma}_{f,\text{in}} \cup \widehat{\Gamma}_{f,\text{out}}, \\ \hat{u}_f &= \hat{u}_s \quad \text{on } \widehat{\Gamma}_i. \end{aligned}$$

The ALE map is constructed by solving a mixed formulation of the biharmonic equation in the sense of Ciarlet [28]. We introduce an auxiliary variable $\hat{\eta} = -\hat{\Delta}\hat{u}$ and obtain two differential equations:

$$\begin{aligned} \hat{\eta} &= -\hat{\Delta}\hat{u} \quad \text{in } \widehat{\Omega}_f, \\ -\hat{\Delta}\hat{\eta} &= 0 \quad \text{in } \widehat{\Omega}_f. \end{aligned} \tag{6}$$

By employing the two equations (6) to construct the ALE mapping, the first equation is defined on all $\widehat{\Omega}$, whereas the second equation is only defined in the fluid domain $\widehat{\Omega}_f$. For more details and a comparison study of different mesh motion techniques, we refer to [14].

Absorbing conditions for the structure

Over the last decade, much effort has been spent on descriptions of appropriate conditions in (artificial) inlet and outlet boundaries (of blood vessels) for fluid and pressure (see [1, 4, 21, 22], and the many references cited therein). Specifically, the fluid-wall interaction is responsible for the propagation of pulse pressure waves in the blood vessel. This is a characteristic issue that only appears in compliant vessels and not in domains with fixed walls.

In our study, we focus on boundary conditions for the blood vessel in the outflow. Often, the vessel structure is fixed in the horizontal direction and left free in the vertical direction [21]. Recently, a first step in addressing structural conditions has been taken in [22]. Here, the authors compare three different strategies by extending methods from the rigid case. However, they apply these strategies to blood vessel computations with moderate deformations but not to heart valve dynamics.

We turn now to interaction processes occurring in heart valve dynamics. A prototypical configuration is sketched in Figure 1. Usually, one would solve the equations by using $\widehat{\Omega}$ and imposing Dirichlet or Neumann conditions on $\widehat{\Gamma}_{i,s}$. For both types of conditions, waves are reflected at the outflow boundary, which is illustrated in Figure 2 for a clamped structure (homogenous Dirichlet conditions) on $\widehat{\Gamma}_{s,out}$.

In our approach, we extend the computational domain by using a well-known technique from acoustics, which is comparable to the perfectly matched layer approach [25].

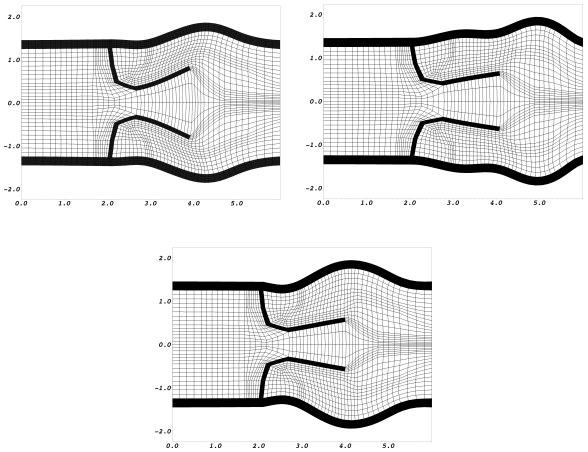

Figure 2 Sequence of states of a reflected wave at the structure outflow boundary at different time steps: incoming waves are displayed in the left and middle figure. The reflected wave is shown in the figure at the bottom.

In the artificial part $\widehat{\Omega}^{ext} = \widehat{\Omega}_f^{ext} \cup \widehat{\Omega}_s^{ext}$ of the computational domain, we prescribe a damped version of the structure equations in $\widehat{\Omega}_s^{ext}$, to absorb outgoing waves and to prevent structure reflections. One drawback of this method is the higher computational cost that results because we solve both the full fluid equations and the structure equations in the artificial layer. However, we coarsen the grid manually in the artificial domain because we are not interested in observing any physical quantity in that domain. Ideally, one would solve reduced models on the artificial domain or coarsen the mesh automatically during the solution process. Here, one could use goal-oriented mesh adaption with the dual weighted residual method (DWR) [16]. A simplified version of the DWR method for a stationary setting for our configuration was tested in [29].

The modified structure problem for the extended domain is defined by:

$$\hat{\rho}_s \partial_t^2 \hat{u}_s - \widehat{\mathrm{div}}(\widehat{F}\widehat{\Sigma}_s(\hat{u}_s)) + \gamma_w \partial_t \hat{u}_s = 0 \quad \text{in } \widehat{\Omega}_s^{ext},$$

with $\gamma_w \geq 0$. Here, the damping term is referred to as *weak damping*.

In the following, we pose a standard mixed formulation for the structure equations,

$$\begin{aligned} \hat{\rho}_s \partial_t \hat{v}_s - \widehat{\mathrm{div}}(\widehat{F}\widehat{\Sigma}_s(\hat{u}_s)) + \gamma_w \hat{v}_s = 0 \quad &\text{in } \widehat{\Omega}_s^{ext}, \\ \hat{\rho}_s \partial_t \hat{u}_s - \hat{v}_s = 0 \quad &\text{in } \widehat{\Omega}_s^{ext}. \end{aligned} \tag{7}$$

The modified structure Equation (7) reduces to the original Equation (2) by setting the damping parameter to $\gamma_w = 0$. Therefore, we are dealing in the following only with Equation (7) in $\widehat{\Omega}_s$, and we omit differentiation between $\widehat{\Omega}_s$ and $\widehat{\Omega}_s^{ext}$.

For structural damping, one could also use a damping form that is related to the entire structural operator. This kind of damping is a so-called *strong damping* and leads to a modification of the interface conditions between the fluid and the structure. This issue is examined in [39].

The variational form in the reference domain

So far, the description is not related to a specific solution algorithm. In this section, we specify our solution framework and formulate the equations in a monolithic setting. The coupling of the equations of Problem 1 with 7 via the conditions in Equation (4) is derived in the same manner as [14]. To this end, all equations are defined (and solved) in the reference configuration $\widehat{\Omega} = \widehat{\Omega}_f \cup \widehat{\Omega}_s$. A continuous variable $\hat{u}$ in $\widehat{\Omega}$, defining the deformation in $\widehat{\Omega}_s$, and supporting the transformation in $\widehat{\Omega}_f$, is defined. Then, we get the standard relations

$$\hat{\mathcal{A}} := id + \hat{u}, \quad \widehat{F} := I + \widehat{\nabla}\hat{u}, \quad \hat{J} := \det(\widehat{F}). \tag{8}$$

Furthermore, the velocity $\hat{v}$ and the additional displacement variable $\hat{\eta}$ are common continuous functions for both subproblems. The pressure $\hat{p}$ should be discontinuous over the interface $\widehat{\Gamma}_i$ because there is no physical relation between $\hat{p}_f$ and $\hat{p}_s$. The problem reads:

Find $\{\hat{v}, \hat{u}, \hat{\eta}, \hat{p}\} \in \{\hat{v}^D + \hat{V}^0\} \times \{\hat{u}^D + \hat{V}^0\} \times \hat{V} \times \hat{L}^0$, such that $\hat{v}(0) = \hat{v}^0$ and $\hat{u}(0) = \hat{u}^0$, for almost all time steps $t \in I$, and

$$\begin{aligned} &(\hat{J}\hat{\rho}_f \partial_t \hat{v}, \hat{\psi}^v)_{\widehat{\Omega}_f} \\ &+(\hat{\rho}_f \hat{J}(\widehat{F}^{-1}(\hat{v} - \hat{w}_f) \cdot \widehat{\nabla})\hat{v}), \hat{\psi}^v)_{\widehat{\Omega}_f} \\ &+(\hat{J}\widehat{\sigma}_f \widehat{F}^{-T}, \widehat{\nabla}\hat{\psi}^v)_{\widehat{\Omega}_f} + (\hat{\rho}_s \partial_t \hat{v}, \hat{\psi}^v)_{\widehat{\Omega}_s} \\ &+(\widehat{F}\widehat{\Sigma}_s, \widehat{\nabla}\hat{\psi}^v)_{\widehat{\Omega}_s} + \gamma_w(\partial_t \hat{u}_s, \hat{\psi}^v)_{\widehat{\Omega}_s} = 0 \quad \forall \hat{\psi}^v \in \hat{V}^0, \\ &(\partial_t \hat{u} - \hat{v}, \hat{\psi}^u)_{\widehat{\Omega}_s} + (\hat{\alpha}_u \widehat{\nabla}\hat{\eta}, \widehat{\nabla}\hat{\psi}^u)_{\widehat{\Omega}_f} = 0 \quad \forall \hat{\psi}^u \in \hat{V}^0, \\ &(\hat{\alpha}_u \hat{\eta}, \hat{\psi}^\eta)_{\widehat{\Omega}} + (\hat{\alpha}_u \widehat{\nabla}\hat{u}, \widehat{\nabla}\hat{\psi}^\eta)_{\widehat{\Omega}} = 0 \quad \forall \hat{\psi}^\eta \in \hat{V}, \\ &(\widehat{\mathrm{div}}(\hat{J}\widehat{F}^{-1}\hat{v}), \hat{\psi}^p)_{\widehat{\Omega}_f} + (\hat{p}, \hat{\psi}^p)_{\widehat{\Omega}_s} = 0 \quad \forall \hat{\psi}^p \in \hat{L}^0, \end{aligned}$$

with $\hat{\rho}_f$, $\hat{\rho}_s$, ν_f, μ_s, λ_s, $\widehat{F}$, $\hat{J}$, and a positive (small) diffusion parameter $\hat{\alpha}_u$. The stress tensors, $\widehat{\sigma}_f$ and $\widehat{\Sigma}_s$, are defined as

$$\begin{aligned} \widehat{\sigma}_f &:= -\hat{p}_f I + \hat{\rho}_f \nu_f (\widehat{\nabla}\hat{v}_f \widehat{F}^{-1} + \widehat{F}^{-T}\widehat{\nabla}\hat{v}_f^T), \\ \widehat{\Sigma}_s^{\mathrm{STVK}} &:= (\lambda_s(\mathrm{tr}\widehat{E})I + 2\mu_s \widehat{E}), \\ \widehat{\sigma}_s^{\mathrm{INH}} &:= -\hat{p}I + \mu_1 \widehat{F}\widehat{F}^T, \end{aligned}$$

where $\widehat{F}\widehat{\Sigma}_s = \hat{J}\widehat{\sigma}_s \widehat{F}^{-T}$ gives the link between the different stress tensor notations.

The viscosity and the density of the fluid are denoted by ν_f and $\hat{\rho}_f$, respectively. The function $\hat{g}$ represents the Neumann boundary conditions for both physical boundaries (e.g., zero stress at the outflow boundary), and normal stresses on $\widehat{\Gamma}_i$. Later, this boundary represents the interface between the fluid and the structure. The structure is characterized by the density $\hat{\rho}_s$ and the Lamé coefficients μ_s, λ_s. For the STVK material, the compressibility is related to the Poisson ratio ν_s ($\nu_s < \frac{1}{2}$).

This problem is completed by an appropriate choice of the two coupling conditions on the interface. The continuity of velocity across $\widehat{\Gamma}_i$ is strongly enforced by requiring one common continuous velocity field on the whole domain $\widehat{\Omega}$. The continuity of normal stresses is given by

$$(\hat{J}\widehat{F}\widehat{\Sigma}_s\widehat{F}^{-T}\hat{n}_s, \hat{\psi}^v)_{\widehat{\Gamma}_i} = (\hat{J}\widehat{\sigma}_f\widehat{F}^{-T}\hat{n}_f, \hat{\psi}^v)_{\widehat{\Gamma}_i}. \quad (9)$$

By omitting this boundary integral jump over $\widehat{\Gamma}_i$, the weak continuity of the normal stresses becomes an implicit condition of the fluid-structure interaction problem.

To ease the notation, the structure stress tensors are considered in the above problem as follows:

$$\widehat{\Sigma} := \sum_i^n \widehat{\Sigma}_i, \quad n = 1, 2, 3,$$

where $\widehat{\Sigma}_i$ denotes the sub-structure tensor of each structural problem.

Discretization

To discretize the non-linear problem, we introduce a semi-linear form and we write the (non-linear) equation system in compact notation: Find $\hat{U} = \{\hat{v}, \hat{u}, \hat{\eta}, \hat{p}\} \in \widehat{X}^0$, where $\widehat{X}^0 := \{\hat{v}^D + \hat{V}^0\} \times \{\hat{u}^D + \hat{V}^0\} \times \hat{V} \times \hat{L}$, such that

$$\int_0^T \hat{A}(\hat{U})(\hat{\Psi})\, dt = \int_0^T \hat{F}(\hat{\Psi})\, dt \quad \forall \hat{\Psi} \in \widehat{X}, \quad (10)$$

where $\widehat{X} = \hat{V}^0 \times \hat{V}^0 \times \hat{L}^0$. The time integral is defined in an abstract sense such that the equation holds for *almost* all time steps. The linear form is given by $\hat{F}(\hat{\Psi}) \equiv 0$ because we neglect volume forces. The semi-linear form $\hat{A}(\hat{U})(\hat{\Psi})$ is defined by

$$\begin{aligned}
\hat{A}(\hat{U})(\hat{\Psi}) = {} & (\hat{J}\hat{\rho}_f\partial_t\hat{v}, \hat{\psi}^v)_{\widehat{\Omega}_f} \\
& + (\hat{\rho}_f\hat{J}(\widehat{F}^{-1}(\hat{v} - \hat{w}) \cdot \widehat{\nabla})\hat{v}), \hat{\psi}^v)_{\widehat{\Omega}_f} \\
& + (\hat{J}\widehat{\sigma}_f\widehat{F}^{-T}, \widehat{\nabla}\hat{\psi}^v)_{\widehat{\Omega}_f} + (\hat{\rho}_s\partial_t\hat{v}, \hat{\psi}^v)_{\widehat{\Omega}_s} \\
& + (\hat{J}\widehat{\sigma}_s\widehat{F}^{-T}, \widehat{\nabla}\hat{\psi}^v)_{\widehat{\Omega}_s} + \gamma_w(\hat{v}, \hat{\psi}^v)_{\widehat{\Omega}_s} \\
& - \langle\hat{g}, \hat{\psi}^v\rangle_{\widehat{\Gamma}_N} + (\hat{\alpha}_u\hat{\eta}, \hat{\psi}^\eta)_{\widehat{\Omega}} \\
& + (\hat{\alpha}_u\widehat{\nabla}\hat{u}, \widehat{\nabla}\hat{\psi}^\eta)_{\widehat{\Omega}} + (\partial_t\hat{u}, \hat{\psi}^u)_{\widehat{\Omega}_s} \\
& - (\hat{v}, \hat{\psi}^u)_{\widehat{\Omega}_s} + (\hat{\alpha}_u\widehat{\nabla}\hat{\eta}, \widehat{\nabla}\hat{\psi}^u)_{\widehat{\Omega}_f} \\
& + (\widehat{\mathrm{div}}\,(\hat{J}\widehat{F}^{-1}\hat{v}), \hat{\psi}^p)_{\widehat{\Omega}_f} + (\hat{p}, \hat{\psi}^p)_{\widehat{\Omega}_s}.
\end{aligned} \quad (11)$$

Temporal discretization is based on finite differences and the one step-θ schemes [34]. We use the shifted Crank-Nicolson scheme based on finite differences that was developed for this ALE scheme in [14]. Spatial discretization in the reference configuration $\widehat{\Omega}$ is treated by a conforming Galerkin finite element scheme, leading to a finite dimensional subspace $\widehat{X}_h \subset \widehat{X}$. The discrete spaces are based on the Q_2^c/P_1^{dc} element for the fluid problem [35]. The structure problem is discretized by the Q_2^c element. The non-linear problem is solved by the Newton method where the Jacobian is derived by exact linearization of the directional derivatives [14]. Here, the linear equations are solved with a direct solver (UMFPACK).

Residual based stabilization for the convective term

Modeling blood flow at the exit of the aortic valve leads to a convection-dominated problem with a Reynolds number of ~ 4500 [30]. For this reason, we must stabilize our formulation. The first ideas on this subject go back to [36]. Our method of choice is the streamline upwind Petrov-Galerkin (SUPG) method. A simplified (non-consistent) version in $\widehat{\Omega}_f$ reads:

$$\begin{aligned}
& s_{\mathrm{SUPG}}(\hat{U}_{kh})(\hat{\Psi}) \\
& := \sum_{m=1}^M \left\{ \int_{I_m} \sum_{\widehat{K} \in \mathcal{T}_h^m} (\hat{\rho}_f(\hat{J}\widehat{F}^{-1}\hat{v}_f \cdot \widehat{\nabla})\hat{v}_f, \delta_{K,m}(\hat{v}_{kh} \cdot \widehat{\nabla}\widehat{F}^{-1})\hat{\psi}^v)_{\widehat{K}} \right\}.
\end{aligned}$$

with

$$\delta_{K,m} = \delta_0 \frac{h_K^2}{6\nu_f + h_K||v_{kh}||_K}, \quad \delta_0 = 0.1.$$

For more details on the choice of these parameters, we refer to [37].

Numerical Tests

To test our proposed method, we set up a prototypical problem. The data for the material parameters and the geometry are taken from the literature [1, 30], and have been discussed with a medical doctor. One cardiac cycle has a time length of $T = [0s, 0.9s]$. Four time cycles are used to run the computation. The time step size k is chosen in the range of $0.02s - 0.001s$ to identify convergence with respect to time. The results are split into three sections. In the first set of computations, we validate the model in a straight channel. Afterwards, we present results for a curved tube, which has a closer geometrical relationship to the 'real' aorta. In the last part, we discuss our results obtained by using different constitutive structure tensors.

Configuration

The (reference) configuration $\widehat{\Omega}$ of the numerical test case is illustrated in Figure 1. Specifically, we set $L^{\text{heart}} + L^{\text{aorta}} = 6.0cm$, $L^{\text{ext}} = 12cm$, $H = 2.9cm$, $D = 2.5cm$, and $d = 0.5cm$. The distance between the two valves was chosen to be sufficiently large to avoid topological difficulties.

Inflow and boundary conditions

A time-dependent parabolic velocity inflow profile is prescribed on $\widehat{\Gamma}_{in}$ (left boundary H), and is sketched in Figure 3. This inflow profile is scaled by a constant factor 0.1. The 'do-nothing' condition is used on $\widehat{\Gamma}_{out}$ (right boundary D).

The structure is clamped on $\widehat{\Gamma}_{in}$ and $\widehat{\Gamma}_{out}$. On the other parts, the structure is left free to allow the walls to move. Specifically, the structure on the outflow boundary of the extended domain is fixed by homogenous Dirichlet conditions. Here, we assume that all reflections have already been absorbed by the damped structure equations.

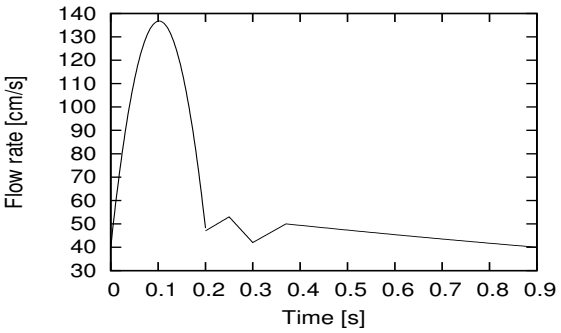

Figure 3 Interpolated flow rate profile in one cardiac cycle, which is imposed at the inflow boundary.

Quantities of comparison and their evaluation

We evaluate the deflections in both the x- and y-directions at the tails of one valve, at the point $A(0) = (3.64, 0.35)$. Moreover, we measure the wall stresses between the fluid and the structure in the upper part of the wall (over the length L^{aorta} at the interface between the fluid and the structure). The upper wall measurement is important in medical engineering applications where high stresses behind the aortic heart valve can lead to an aortic dissection. We measured the minimal (min), maximal (max), and amplitude (ampl) values.

Parameters

For the fluid, we use the density $\rho_f = 1gcm^{-3}$, and the viscosity $\nu_f = 0.03cm^2s^{-1}$. The elastic structure is characterized by the density $\rho_s = 1gcm^{-3}$, the Poisson ratio $\nu_s = 0.3$, and the Lamé coefficients $\mu_{heart} = 10^8gcm^{-1}s^{-2}$, $\mu_{valve} = 5.0 * 10^5gcm^{-1}s^{-2}$, $\mu_{aorta} = 10^6gcm^{-1}s^{-2}$. The (weak) damping parameter is given by $\gamma_w = 10^4$.

Results for valve dynamics in a straight channel

The results indicate that our proposed model is suitable to run valve dynamics for a prototypical configuration. We show at least two time levels and three mesh levels to identify convergence with respect to time and space, respectively. The results of the physical quantities are summarized in [38, 39]. The qualitative behavior of the quantities of interest for the last three cycles can be observed in Figure 4.

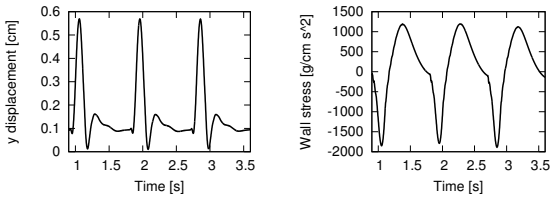

Figure 4 Evaluation of the x and y displacements (top) and wall stresses in the x and y-directions (bottom) for the valve dynamics in a straight channel.

We show the qualitative behavior of the results in the Figure 5. If the damping parameter is too low, structure waves propagate through the whole structure domain. On the other hand, if the damping parameter chosen is too high, the structure becomes too stiff and outgoing waves are reflected.

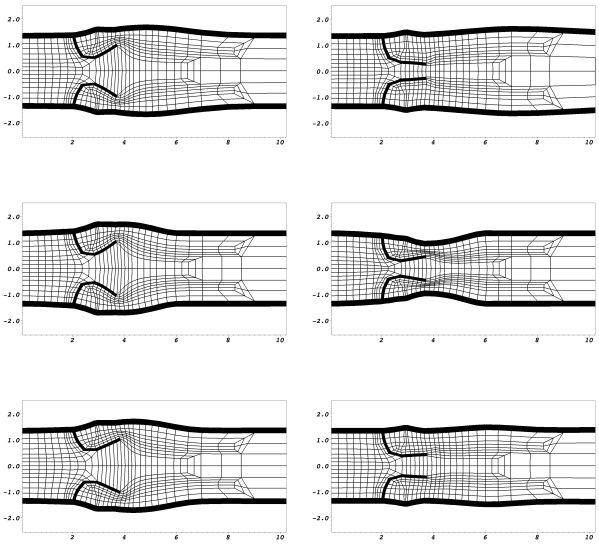

Figure 5 Valve simulations in a straight channel with too low damping $\gamma_w = 10^3$ (top), with too strong damping $\gamma_w = 10^6$ (middle), and with proper damping $\gamma_w = 10^4$ (bottom).

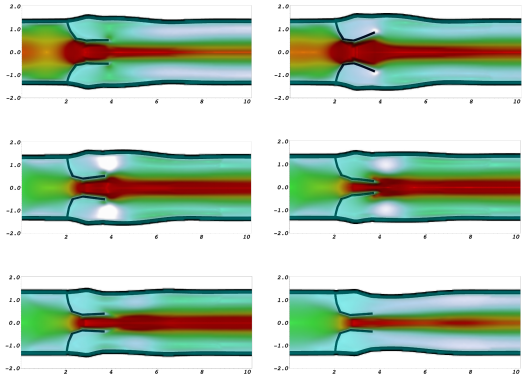

Figure 6 From the left to the right and from the top to the bottom: time sequence of solutions of the x-velocity to the non-stationary valve simulations within one cardiac cycle. The highest velocity is indicated in red. Fluid back flow is indicated in light blue, caused by compliance of the vessel walls and the incompressibility of the fluid.

Results for valve dynamics in a curved channel

This example is a slight modification of the previous example; here, the geometry has a closer relation to a 'real' blood vessel (see Figure 7). The qualitative behavior of the quantities of interest is comparable to the results of the straight channel, which is illustrated in Figure 8.

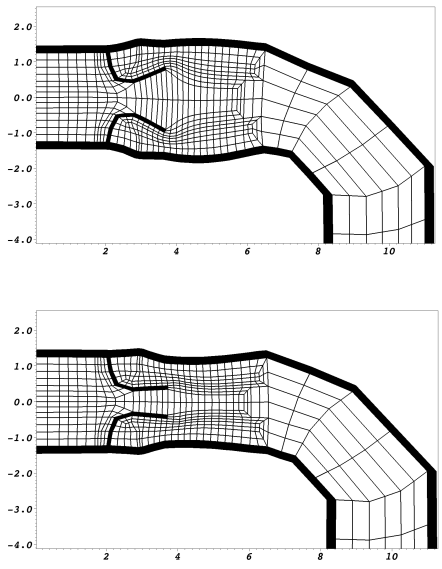

Figure 7 Valve simulations in a curved domain with proper damping $\gamma_w = 10^4$.

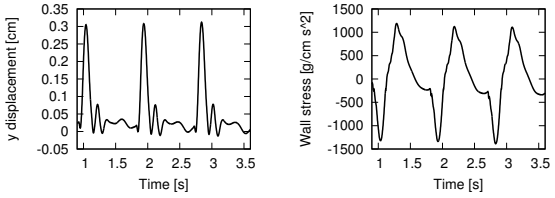

Figure 8 Evaluation of the x and y displacements (top) and the wall stresses in the x and y directions (bottom) for the curved configuration.

Results for valve dynamics with multiple structures

Up to now, the structure was described by the same structure model, namely the STVK material, but with varying coefficients. In this numerical example, we test our solution algorithm with different structure models, where the stress tensor changes entirely. Here, the heart section L^{heart} and the leaflets are modeled by the INH material. The aorta L^{aorta} and the artificial structure L^{aorta} are still described by the STVK material.

The purpose of this example is twofold:

- Do we observe any difficulties of our monolithic solution algorithm? This is question is important with regard to the following task (see future ideas). The structure of blood vessel walls is a highly complex composition of different materials with constitutive stress tensors and different properties. Thus, we make a first step in this work, to compute a fluid-multi-structure system.
- Second, do we detect different behavior for the quantities of interest?

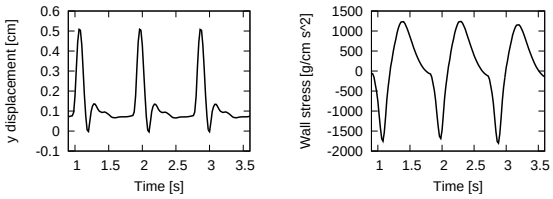

Figure 9 Evaluation of the y displacement (left) and the wall stress in the y-direction (right) for the valve dynamics with multiple structures in a straight channel.

To respond to the first question, we observed that the convergence of Newton's method at each time step was slightly better, while in-cooperating the multi-structure model. This result indicate that the solution algorithm performs better when modeling the valves and the heart section by the INH material. This is in agreement with our observations of the comparison in [39]. There, we observed a failure (and bad convergence of the Newton method) of the STVK material for large deflections. In the present test case, we observe again bad convergence of the STVK material for large deflections.

Second, we observe the same qualitative (nearly the identical) behavior for all quantities of interest (see Figure 9). This was expected for the wall stresses because we still used the STVK material in L^{aorta}.

Conclusions

In this work, we proposed a monolithic fluid-structure framework to simulate two-dimensional long axis valve dynamics on prototypical configurations. Here, we were concerned with large structural deformations of the blood vessel. To overcome difficulties with reflected structure waves at the outflow boundary, we solved damped hyperbolic equations on a prolongated domain. In further studies, we plan to investigate the influence of strong and weak damping parameters. Second, we plan to couple the model with absorbing boundary conditions for the fluid part that accounts for wave propagations. Third, we will incooperate sophisticated structure equations to modeling arterial tissue.

Acknowledgments

The financial support by the DFG (Deutsche Forschungsgemeinschaft) and the HGS MathComp Heidelberg is gratefully acknowledged. Further, the author thanks Jeremi Mizerski for discussing details on the models; Rolf Rannacher, Alexandra Moura and Adelia Sequeira for fruitful discussions on boundary conditions.

References

[1] A. Quarteroni, What mathematics can do for the simulation of blood circulation, *MOX Report* (2006).

[2] C.A. Figueroa, I.E. Vignon-Clementel, K.E. Jansen, T.J.R. Hughes, C.A. Taylor, A coupled momentum method for modeling blood flow in three-dimensional deformable arteries. *Comput. Methods Appl. Mech. Engrg.* **195**, pp. 5685–5706 (2006)

[3] F. Nobile, C. Vergara, An Effective Fluid-Structure Interaction Formulation for Vascular Dynamics by Generalized Robin Conditions. *SIAM J. Sci. Comput.* **30**(2), pp. 731–763 (2008)

[4] J. Janela, A. Moura, A. Sequeira, Absorbing boundary conditions for a 3D non-Newtonian fluid-structure interaction model for blood flow in arteries. *Int. J. Engrg. Sci.* (2010).

[5] Z. Jianhai, C. Dapeng, Z. Shengquan, ALE finite element analysis of the opening and closing process of the artificial mechanical valve. *Appl. Math. Mech.* **17**(5), pp. 403–412 (2006)

[6] P. Le Tallec, J. Mouro, Fluid structure interaction with large structural displacements. *Comput. Meth. Appl. Mech. Engrg.* **190**, pp. 3039–3067 (2001)

[7] C. Peskin, The immersed boundary method. *Acta Numerica - Cambridge University Press*, pp. 1–39 (2002)

[8] N. Diniz Dos Santos, J.F. Gerbeau, J.F. Bourgat, A partitioned fluid-structure algorithm for elastic thin valves with contact. *Comp. Meth. Appl. Mech. Engrg.* **197**(19–20), pp. 1750-1761 (2008)

[9] J. Vierendeels, K. Dumont, P.R. Verdonck, A partitioned strongly coupled fluid-structure interaction method to model heart valve dynamics. *J. Comp. Appl. Math.* (2008)

[10] J. Hron, S. Turek, A monolithic FEM/Multigrid Solver for an ALE formulation of fluid-structure interaction with applications in biomechanics. *In Fluid-Structure Interaction: Modeling, Simulation, Optimization. Lecture Notes in Computational Science and Engineering*, Vol. **53**, pp. 146–170, Bungartz, Hans-Joachim; Schafer, Michael (Eds.), Springer (2006)

[11] M. A. Fernandez, J.F. Gerbeau. Algorithms for fluid-structure interaction problems. In *Cardiovascular Mathematics: Modeling and simulation of the circulatory system.* Springer-Verlag, Italia, Milano (2009)

[12] H.-J. Bungartz, M. Schäfer, *Fluid-Structure Interaction II: Modelling, Simulation, Optimization*. Springer Series: Lecture Notes in Computational Science and Engineering (2010)

[13] T. Richer, T. Wick, Finite elements for fluid-structure interaction in ALE and fully Eulerian coordinates. *Comput. Meth. Appl. Mech. Engrg.* **199**, pp. 2633–2642 (2010)

[14] T. Wick, Fluid-Structure Interactions using Different Mesh Motion Techniques. *Comput. Struct.* **13-14**, pp. 1456–1467 (2011)

[15] P. Causin, J.F. Gerbeau, F. Nobile, Added-mass effect in the design of partitioned algorithms for fluid-structure problems. *Comput. Methods Appl. Mech. Engrg.* **194**, pp. 4506–4527 (2005)

[16] R. Becker, R. Rannacher, An optimal control approach to error control and mesh adaptation in finite element methods. *Acta Numerica 2001 (A. Iserles, ed.), Cambridge University Press* (2001)

[17] R. Glowinski, T.W. Pan, T.I. Hesla, J. Périaux, A fictitious domain method for dirichlet problem and applications. *Comput. Meth. Appl. Mech. Engrg.* **111**, pp. 283–303 (1994)

[18] J. Heywood, R. Rannacher, S. Turek, Artificial boundaries and flux and pressure conditions for the incompressible Navier-Stokes equations. *Int. J. Num. Meth. Fluids.* **22**, pp. 325–353 (1996)

[19] L. Formaggia, A. Quarteroni, A. Veneziani, *Cardiovascular Mathematics: Modeling and simulation of the circulatory system.* Springer-Verlag, Italia, Milano (2009)

[20] L. Formaggia, J.F. Gerbeau, F. Nobile, A. Quarteroni, On the Coupling of 3D and 1D Navier-Stokes equations for Flow Problems in Compliant Vessels. *Comput. Meth. Appl. Mech. Engng.* **191**, pp. 561–582 (2001)

[21] L. Formaggia, A. Moura, F. Nobile, On the stability of the coupling of 3D and 1D fluid-structure interaction models for blood flow simulations. *Technical Report MOX* **94** (2006).

[22] L. Formaggia, A. Veneziani, Ch. Vergara, Flow rate boundary problems for an incompressible fluid in deformable domains: formulations and solution methods. *Comput. Meth. Appl. Mech. Engrg.* **199**, pp. 677–688 (2010)

[23] W. Bangerth, M. Grothe, Ch. Hohenegger, Finite element method for time dependent scattering: nonreflecting boundary conditionm, adaptivity, and energy decay. *Comput. Meth. Appl. Mech. Engng.*, **193**, pp. 2453–2482 (2004)

[24] B. Engquist, A. Majda, Absorbing boundary conditions for the numerical simulation of waves. *Math. Comp.* **31**(139), pp. 629–651 (1977)

[25] J.P. Berenger, A perfectly matched layer for the absorption of electromagnetic waves. *J. Comput. Phys.* **114**(184) (1994)

[26] W. Bangerth, R. Hartmann, G. Kanschat, Differential Equations Analysis Library. *Technical Reference* (2010) `http://www.dealii.org`.

[27] J. Wloka, Partielle Differentialgleichungen. *B.G. Teubner*, Stuttgart (1984)

[28] P.G. Ciarlet, P.A. Raviart, A mixed finite element method for the biharmonic equation. Mathematical Aspects of Finite Elements in Partial Differential Equations. (C.de Boor, Eds.), *Academic Press*, New York, pp. 125–145 (1974)

[29] T. Wick, Adaptive Finite Elements for Monolithic Fluid-Structure Interaction on a Prolongated Domain:

Applied to an Heart Valve Simulation, CMM May 9-12, 2011, *Comput. Meth. Mech.*, Warsaw Poland (2011)

[30] Y.C. Fung, Biodynamics: Circulation, first ed., Springer-Verlag (1984)

[31] G.A. Holzapfel, Nonlinear Solid Mechanics, *John Wiley* (2000)

[32] G.A. Holzapfel, R. W. Ogden Mechanics of Biological Tissue, *Springer Heidelberg* (2006)

[33] J. Mizerski, Heart Valve Modeling, *Personal correspondance to the author* (2010)

[34] S. Turek, S., Efficient solvers for incompressible flow problems, *Springer-Verlag* (1999)

[35] V. Girault, P.-A. Raviart, Finite Element Methods for the Navier-Stokes Equations, *Springer, Heidelberg* (1986)

[36] A.N. Brooks, T.J.R. Hughes, Streamline upwind/Petrov-Galerkin formulations for convection dominated flows with particular emphasis on the incompressible Navier-Stokes equations. *Comput. Methods Appl. Mech. Engrg.* **32**(1–3), pp. 199–259 (1982)

[37] M. Braack, E. Burman, V. John, G. Lube, Stabilized finite element methods for the generalized Oseen equations. *Comput. Methods Appl. Mech. Engrg.* **196**(4–6), pp. 853–866 (2007)

[38] T. Wick, Energy absorbing layer for the structure outflow boundary in Fluid-structure interaction for heart valve dynamics. *submitted to a journal* (2011)

[39] T. Wick, Adaptive Finite Element Approximation of Monolithically-Coupled Fluid-Structure Interaction Problems *PhD Thesis*, in preparation (2011)